56th 3AF International Conference on Applied Aerodynamics
28 – 30 March 2022, Toulouse - France

FP70-AERO2022-ignatowicz

DATA-DRIVEN CALIBRATION OF RANS HEAT TRANSFER PREDICTION ON A CURVED ROUGH SURFACE

Kevin Ignatowicz [(1)], François Morency [(2)], Héloïse Beaugendre[(3)] and Elie Solaï[(4)]
[(1)] École de technologie supérieure, 1100, rue Notre-Dame Ouest, Montréal, QC, H3C 1K3, Email: kevin.ignatowicz.1@ens.etsmtl.ca
[(2)] École de technologie supérieure, 1100, rue Notre-Dame Ouest, Montréal, QC, H3C 1K3, Email: francois.morency@etsmtl.ca
[(3)]INRIA, Bordeaux INP, 200, avenue de la Vieille Tour, 33405 Talence, France, Email: heloise.beaugendre@math.u-bordeaux.fr
[(4)]INRIA, Bordeaux INP, 200, avenue de la Vieille Tour, 33405 Talence, France, Email: elie.solai@inria.fr

ABSTRACT

For heat transfer predictions using RANS simulations, turbulence models require adjustments for rough surfaces. The drawback of these adjustments is the tendency to over predict the heat transfers compared to experiments. These over predictions require the use of an additional thermal correction model to lower the heat transfers. Inputting in the correction model the numerical parameters giving the best fit with experimental results is non-trivial, since actual roughness patterns are often irregular. The objective of the paper is to develop a methodology to calibrate two thermal correction models for a rough curved channel test case. First, a design of experiments of heat transfers is built, then metamodels are generated. Finally, the metamodels are used by a Bayesian inversion procedure estimating the best set of input parameters allowing fitting the experimental results. This methodology allows obtaining less than 7% of average discrepancy between the RANS prediction and the experimental results.

1. INTRODUCTION

The numerical simulation of airflow on a rough surface is a challenge. The surface roughness creates a different near-wall behaviour, especially for the skin friction and the heat transfers, compared to a smooth surface. This led to the modification of the classical turbulence models to take into account the roughness elements, like in [1] for the Spalart-Allmaras model. The main feature of the rough extension of the Spalart-Allmaras model resides in setting a non-zero turbulence viscosity at the wall. Usually, these adapted models are designed to predict the correct skin friction coefficient based on experimental benchmark test cases. This focus on the skin friction coefficient alone has a drawback: the heat fluxes are overestimated compared to experimental results. An additional thermal correction model is thus required to adjust the heat flux. To correct the heat flux behaviour, [2] suggested increasing the turbulent Prandtl number close to the wall. Further thermal correction model developments carried out by [3] and recently by [4] kept aiming at a turbulent Prandtl increase.

The thermal correction models take as input several parameters describing the roughness pattern of the surface. These parameters can be physical, such as the roughness height, or numerical, such as the equivalent roughness. The thermal correction of [3], called HAX in this paper, takes 3 input parameters and the 2-Parameter Prandtl correction (2PP) of [4], takes 2. The previous works highlighted that the heat flux is sensitive to those parameters and to the thermal correction model itself [5]. Therefore, the roughness parameters to input in the model to obtain the same heat flux prediction change depending on the thermal correction model. Usually, the link between the roughness height and the equivalent roughness is computed using classical empirical correlations such as [6]. Those correlations were built using manufactured regular roughness patterns, such as regularly spaced cones or hemispheres. In many practical situations, for example in aircraft icing [7], roughness patterns are irregular and present several uncertainty. Therefore, classical empirical correlations can fail to correctly describe an actual roughness pattern in such situations.

To avoid the dependence to empirical correlations in rough heat transfer simulations, a data-driven approach can be used, ensuring that experimental data are available. Machine learning and data-driven techniques have already been successfully applied in CFD, for example for the calibration of turbulence model's constants in [8], highlighting its potential.

Usually, the data-driven approach and uncertainty quantification analysis use metamodels to represent a

complex model. In the CFD field, a metamodel can estimate an output of interest in a quick manner, without the need for running a complete, and time-consuming, CFD simulation. One of the most common metamodel families is the polynomial chaos expansion (PCE) [9]. PCE metamodels were successfully applied in CFD applications over the past decade, for example in [10]. The metamodels can also be useful to calibrate a model with uncertain parameters. The Bayesian inversion is a commonly used tool allowing model calibration and fine-tuning of numerical parameters [11]. This calibration methodology was already used in CFD in the context of turbulence models' constants tuning [12].

The objective of this paper is to set up a methodology to calibrate the roughness parameters to input in the HAX and 2PP thermal correction models to match experimental results of a given test case. More specifically, a rough curved channel geometry, inspired by [2], is used to set up a design of experiments (DOE) of heat transfers. Next, the DOE allows the generation of PCE metamodels. The next step is the sensitivity study, allowing through the Sobol indexes to identify the most sensitive parameters. Finally, the PCE metamodels are used in a Bayesian inversion calibration procedure to calibrate the roughness input parameters with the aim of retrieving the experimental heat transfer distribution in the curved channel.

First, the test case geometry and setup will be described. Second, the HAX and 2PP thermal correction models are detailed, highlighting the role of the roughness parameters in the simulation. Next, the DOE construction is depicted prior to the description of the PCE metamodeling, the sensitivity study and the Bayesian inversion procedures. Finally, the results are shown for both HAX and 2PP thermal correction models, with less than 7% of average discrepancy after calibration compared to the experimental results.

2. TEST CASE GEOMETRY AND SETUP

This section will give details about the geometry used in the present study, along with the RANS setup to perform the flow simulation.

2.1. Physical geometry and boundary conditions

The geometry used to apply the calibration work discussed in this paper is a curved channel inspired by the study of [2]. More specifically, the zone of interest is the rough bottom floor of the channel where the heat transfer coefficient will be monitored. Fig. 1 illustrates the physical geometry.

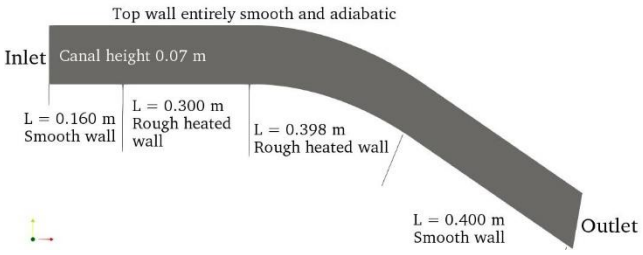

Figure 1. Geometry of the curved channel (out of scale figure for better visualization)

The curved part of the channel's floor, which curvilinear length is 0.398 m, is an arc of radius 1.200 m and angle 19°. The freestream values are a velocity of magnitude 40 m/s, an inlet total pressure of 102 304 Pa and a total temperature of 288.95 K. The boundary conditions are also displayed on Fig. 1. The floor is divided into three main zones: an initial smooth and unheated wall, the rough and heated study zone (including the curved portion), and a downstream smooth unheated zone. The top wall is entirely smooth and adiabatic on the full length. The heated zones are isothermal at 303.15 K and their roughness parameters will vary all along the procedure, since they are the objective of the calibration. The roughness parameters' distribution will be detailed in section 4.

2.2. Mesh and numerical setup

The geometry is discretized using quadrilateral elements in a structured mesh. The rough zone of interest is composed of 499 nodes in the stream-wise direction, while the canal height has 399 elements. Coarser meshes were tested, giving similar results on the benchmark test cases. The finest mesh was retained to cope with the various untested roughness patterns planned to be run during the sampling of the DOE. The entire computational grid has 274 512 quadrilaterals. The first cell height is about 3 µm, which allows a y^+ below 1 for all the roughness ranges tested. The growth rate normal to the wall is 1.1. The flow simulation is performed using the compressible RANS solver SU2 [13]. The Reynolds number based on the total floor length is 3.2 million and the Mach number is 0.118. To accelerate the convergence, the CFL number is set to 10. Finally, the convective fluxes are discretized using a Roe scheme with MUSCL reconstruction. The solver used includes in-house implementations of the rough modification of the Spalart-Allmaras turbulence model [1] and the addition of the HAX [3] and 2PP [4] thermal correction models. The next section will detail the mathematical models making the thermal correction models.

3. THERMAL CORRECTION MODELS

This section will give an overview of the equations of the thermal correction models. Both the HAX and 2PP thermal correction models were implemented into SU2, and aim at increasing the Prandtl number in the near-wall region to lower the heat flux when the rough version of the Spalart-Allmaras turbulence model is used.

3.1. HAX thermal correction model

The HAX thermal correction model suggested by Aupoix increases the turbulent Prandtl number by a value ΔPr_t and takes 3 input parameters describing the roughness pattern: the roughness height k, the equivalent roughness k_s and a surface correction parameter S_{corr}. For recall, all these 3 parameters are the objective of the current calibration work. The value of ΔPr_t is computed with Eq. 1 as follows.

$$\Delta Pr_t = (A(\Delta u^+)^2 + B\Delta u^+)\exp(-d/k) \quad (1)$$

In Eq. 1, the terms and symbols involved are given by Eqs. 2-4.

$$A = (0.0155 - 0.0035S_{corr})(1 - e^{-12(S_{corr}-1)}) \quad (2)$$

$$B = -0.08 + 0.25e^{-10(S_{corr}-1)} \quad (3)$$

$$\Delta u^+ = \frac{1}{\kappa \cdot \log\left(1 + \frac{k_s \cdot u_\tau}{\nu \cdot \exp(1.3325)}\right)} \quad (4)$$

Finally, d is the distance to the wall, κ is the Von Kármán constant, ν is the kinematic viscosity of air and u_τ is the friction velocity.

3.2. 2PP thermal correction model

The 2PP thermal correction model achieves the same goal of increasing the turbulent Prandtl number by ΔPr_t. This time, the model takes only 2 roughness input parameters: the roughness height k, the equivalent roughness k_s. Eq. 5 allows the computation of ΔPr_t.

$$\Delta Pr_t = g \times 0.07083 \times {Re_s}^{0.45} \times Pr^{0.8} \times exp\left(-\frac{d}{k}\right) \quad (5)$$

The roughness Reynolds number and the parameter g in Eq. 5 are detailed in Eqs. 6-7.

$$Re_S = \frac{u_\tau k_s}{\nu} \quad (6)$$

$$g = 1 \text{ if } Re_s \geq 70$$

$$g = \frac{\ln(Re_s) - \ln(5)}{\ln(70) - \ln(5)} \text{ if } 5 < Re_s < 70 \quad (7)$$

$$g = 0 \text{ if } Re_s \leq 5$$

Finally, Eq. 1 and Eq. 5 highlighted that the roughness parameters have a direct impact on the Prandtl number correction, and thus on the predicted heat flux.

4. PCE METAMODELING

This section will depict the metamodeling process retained, using polynomial chaos expansion (PCE) models. This step allows creating metamodels to predict the heat flux behaviour above any roughness pattern without the need for a complete CFD run. The first step of the metamodeling task is the creation of a numerical DOE. The PCE metamodels are then generated, and finally their accuracy is checked to ensure they are reliable enough for the study.

4.1. Design of Experiment (DOE)

To prepare the metamodeling and Bayesian inversion steps, a numerical DOE of heat transfers for various roughness patterns is needed. First, the distribution of the input parameters k, k_s/k and S_{corr} are defined to set the limits of the sampling. Note that the ratio k_s/k is used instead of k_s alone, since it will allow to directly evaluate the link between the roughness height and the equivalent roughness. The present work is included in the broader scope of aircraft icing. Therefore, the typical ranges of variation of k and k_s/k are obtained from the icing literature [14, 15]. Finally, the distribution of the S_{corr} parameter, only used for the HAX thermal correction model, is obtained from [3]. The compilation of the distribution of all the input parameters is given in Tab. 1.

Table 1. Distribution of the input parameters

Parameter	Minimum	Maximum	Distribution
k (mm)	0.41	4.32	Uniform
Ratio k_s/k	0.2	6.5	Uniform
S_{corr}	1	2.5	Uniform

Following the distributions of Tab. 1, a sampling is done (one for 2PP and one for HAX) using the Latin hypercube sampling [16]. The sample size is defined according to the literature [17] for a response surface and gives, with an oversampling factor, 120 samples for the 2-parameters 2PP thermal correction and 190 samples for the three parameters HAX thermal correction.
Following the sampling, 120 CFD simulations of the curved channel are run with the 2PP thermal correction model, and 190 with the HAX thermal correction model. This allows the construction of a numerical heat transfer database, needed for the next metamodeling step.

4.2. Metamodels generation

Once the heat transfer DOE is set up, the metamodeling tool uses it to estimate a mathematical relation between the roughness parameters inputs and the heat flux output.

For this study, polynomial chaos expansion (PCE) metamodels are chosen [9]. The choice of this type of metamodel is motivated by its wide use in uncertainty quantification, including in CFD and aerodynamic applications [18]. The general form of a PCE metamodel is given by Eq. 8.

$$Y_i = M_i(X) = \sum_{\alpha} y_\alpha \times \psi_\alpha(X) \tag{8}$$

In Eq. 8, Y_i is the output of interest, M_i is its corresponding PCE metamodel defined by its coefficients y_α and the polynomials ψ_α of the decomposition. For this study, the PCE metamodels obtained have an order typically between 7 and 10. Two metamodels are generated, as listed in Tab. 2 where h_c is the heat transfer coefficient.

Table 2. Metamodels created

Metamodel	Input parameters HAX	2PP	Output of interest
M_1	k, k_s/k, S_{corr}	k, k_s/k	h_c at the starting point of the rough zone (W/m²K)
M_2	k, k_s/k, S_{corr}	k, k_s/k	Mean relative error with experimental h_c (%)

The first metamodel M_1 uses the DOE to give a PCE prediction of the value of the heat transfer coefficient at the very beginning of the rough zone of study. The second metamodel, M_2, predicts the mean relative error compared to the experimental results of [2]. For M_2, the absolute relative error is computed on each mesh point (where the experimental value is interpolated) and an average is computed.

Once a metamodel is created, its evaluation on the inputs of the DOE allows comparing its prediction with the actual CFD prediction obtained when setting up the DOE. Doing a linear regression between the PCE prediction and the CFD output allows computing the R^2 coefficient (Eq. 9).

$$R^2 = 1 - \frac{\sum(Y_{CFD} - Y_{PCE})^2}{\sum(Y_{CFD} - \bar{Y}_{CFD})^2} \tag{9}$$

In Eq. 9, Y_{CFD}, and Y_{PCE} are the CFD and PCE predictions, respectively. $\bar{Y}_{CFD}$ is the mean value of the output of interest (CFD). An R^2 coefficient close to 1 ensures a PCE metamodel with a good accuracy, since it predicts outputs close to what the full CFD simulation has given. Once the metamodels are established, the next step is to use them for the sensitivity study and calibration purposes.

5. SENSITIVITY STUDY

The sensitivity study allows identifying the most sensitive parameter(s) in the model. Using the previously described PCE metamodels, the sensitivity analysis computes the Sobol indexes, described in [19]. These indexes allow classifying the input parameters from the most to the least sensitive. For input parameters i and j, the first and second order Sobol indexes are defined by Eq. 10 and Eq. 11, respectively.

$$S_i = \frac{V(Y) - E(V(Y|X_i))}{V(Y)} \tag{10}$$

$$S_{i,j} = \frac{V(Y) - E(V(Y|X_i, X_j))}{V(Y)} \tag{11}$$

In Eqs. 10-11, Y is the output of interest, V is the variance, E the mean value, and the notation $Y|X_i$ denotes the output of interest when the ith input parameter is fixed. Finally, the total Sobol index, which is monitored in the present study, for the ith input parameter for a generic three parameters study is given by Eq. 12.

$$S_{Ti} = 1 - (S_j + S_k + S_{j,k}) \tag{15}$$

The greater is the total Sobol index value, the most sensitive to the output of interest is the corresponding input parameter.

6. BAYESIAN INVERSION CALIBRATION

Observing experimental results without an a priori knowledge of the roughness pattern is not helpful to precisely extract the roughness parameters. This task is even more non-trivial since the roughness parameters to input in the model vary depending on the thermal correction model chosen. The calibration is intended to estimate those roughness parameters by working on the PCE metamodels previously created.

For this purpose, the Bayesian inversion technique is used [11]. By inputting the experimental observation (i.e., starting value of h_c for metamodel M_1 or zero for the metamodel M_2), the roughness parameters that best fit the observations are computed. The distribution of the roughness parameters is the same as the one used to generate the CFD DOE (Tab. 1). The framework for this Bayesian inversion is the UQLab tool. The Bayesian module of UQLab uses a Markov chain Monte-Carlo (MCMC). The samplers used in the study are the affine invariant ensemble algorithm (AIES) or the Metropolis-Hastings (MH) algorithm. For the purposes of the work, the MCMC solver is tuned to perform 70 000 iterations and generates 15 chains. When using the PCE metamodels, the error between the metamodel output and the true CFD response is called the discrepancy. The discrepancies of the metamodels being a priori unknown,

their distributions are assumed to be uniform. The range of discrepancy for the metamodel M_1 is from 0 W/m²K to 15 W/m²K and from 0% to 5% for metamodel M_2.
The Bayesian inversion step outputs the calibrated roughness parameters, which are then run into the full CFD solver. The results are then compared with the experimental literature, to assess the success of the calibration.

7. RESULTS

This section will display the results obtain all through the process described in the previous sections. First, the CFD results obtained initially before calibration are shown to illustrate the baseline results. Next, the set of heat transfer coefficients composing the sampling DOE is plotted. The precision of the metamodels is then assessed prior to the display of the final calibrated results.

7.1. CFD results before calibration

Prior to the metamodeling and calibration process, the curved channel test case, as described in section 2.1, is run alone to verify the CFD settings and mesh. A mesh convergence study, not presented in this paper for concision, was carried out successfully to validate the choice of the mesh. These initial simulations, called here the baseline simulations, are run once with the 2PP thermal correction and once with the HAX thermal correction. The experimental roughness pattern being a priori unknown, generic usual roughness parameters are set in the solver for these baseline simulations. The link between the roughness height and the equivalent roughness is done with the Dirling correlation. These assumptions give k = 0.5 mm, k_s = 1.55 mm and for the HAX thermal correction, S_{corr} = 1.05. The heat transfer results obtained with these settings are plotted on Fig. 2.

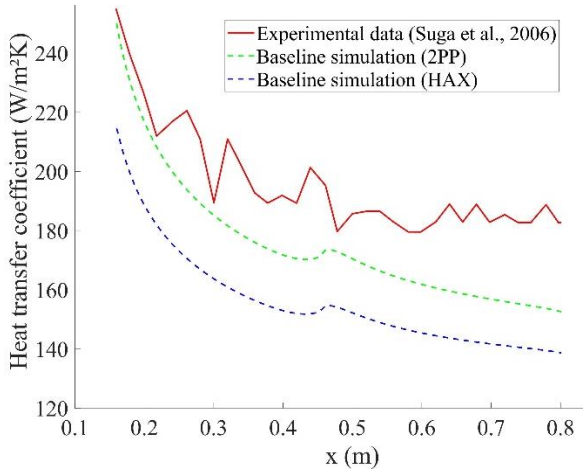

Figure 2. Baseline results before calibration

From Fig. 2, it is possible to notice a relatively poor agreement with the literature. Actually, finding the best roughness parameters is non-trivial, and it legitimates the use of the data-driven calibration approach.

7.2. Visualization of the DOE outputs

After a sampling of the roughness parameters with the Latin hypercube method, 120 CFD simulations with the 2PP thermal correction and 190 with the HAX thermal correction are run. The heat transfer databases obtained from the DOE are plotted in Fig. 3 for the 2PP correction and in Fig.4 for the HAX correction. On both Figs. 2-3, the experimental data from the literature are shown.

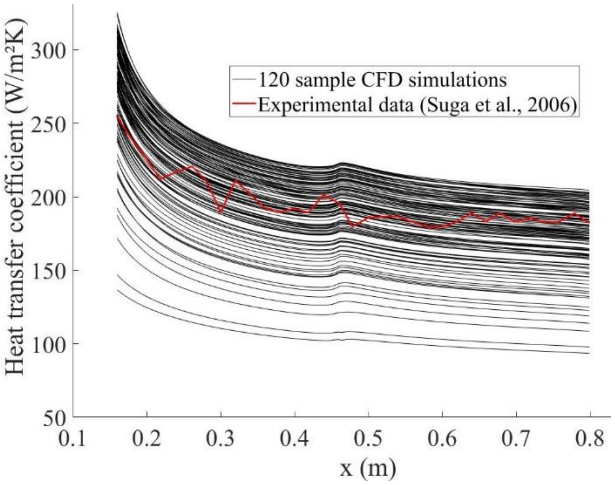

Figure 3. Database of heat transfer coefficients for 2PP correction obtained with the DOE

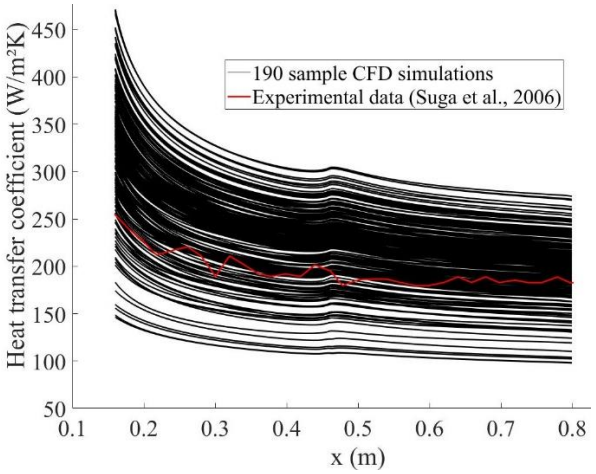

Figure 4. Database of heat transfer coefficients for HAX correction obtained with the DOE

Figs 3-4 show that the target experimental results are included in the envelopes defined by the sampling CFD simulations. This observation shows that the initial range of roughness parameters chosen contains the experimental (a priori unknown) values. By comparing Fig. 3 and Fig. 4, it is possible to see that the HAX thermal correction model predicts overall higher heat

transfer coefficients than the 2PP thermal correction. The envelope of values for HAX is between 150 W/m²K and 450 W/m²K at the beginning of the zone, while it is between 140 W/m²K and 330 W/m²K for the 2PP thermal correction.

7.3. Accuracy of the metamodels

The previous DOE is used as a basis for the PCE metamodel generation. Two metamodels are generated: one to predict the initial value of h_c along the rough zone, and one to predict the mean relative error with experimental results (see Tab. 2). For each metamodel and each thermal correction model, the R² coefficient is calculated (see Eq. 9). The R² values obtained are gathered in Tab. 3.

Table 3. R² coefficient for each metamodel

Metamodel	Output of interest	R² coefficient	
		HAX	2PP
M_1	h_c at the starting point of the rough zone (W/m²K)	0.99949	0.99994
M_2	Mean relative error with experimental h_c (%)	0.99673	0.99962

Tab. 3 shows that all regression coefficients are above 99.6%, meaning an excellent agreement between the CFD results and the PCE-predicted results on the same sample. For comparison, [20] performed the same type of uncertainty quantification analysis with R² coefficients as low as 94.6%. For graphical visualization, the worst regression (M_2/HAX, with R² of 99.673%) is plotted on Fig. 5 where Y_{PCE} and Y_{CFD} are the mean errors in percentage with the literature, as predicted by PCE and CFD respectively.

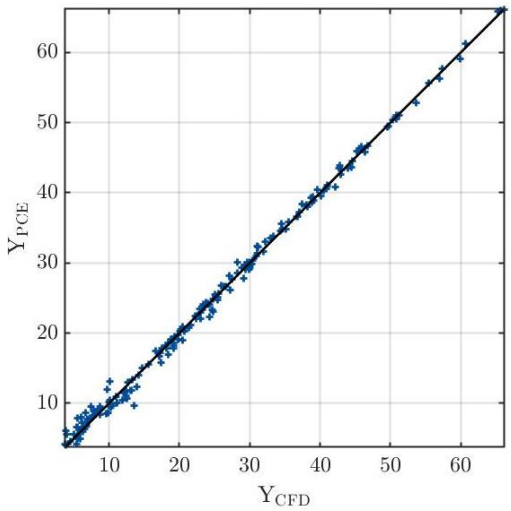

Figure 5. Regression between PCE and CFD predictions (M_2/HAX)

Fig. 5 shows that the results are close to the identity line, visually confirming the good value of the R² regression coefficient. This R² assessment shows that the metamodels generated are accurate and reliable enough to be used in the present application.

7.4. Sensitivity study

Using the PCE metamodels, the sensitivity allows computing the Sobol sensitivity indexes. Tab. 4 gathers the total Sobol index values for each metamodel and thermal correction model.

Table 4. Total Sobol indexes

Metamodel	Total Sobol index	
	HAX	2PP
M_1	k: 0.1570 k_s/k: 0.4337 S_{corr}: 0.4608	k: 0.1445 k_s/k: 0.8868
M_2	k: 0.2196 k_s/k: 0.4955 S_{corr}: 0.6172	k: 0.3061 k_s/k: 0.9772

Tab. 4 shows that the roughness height k is the least sensitive parameter in each case, with a total index between 14% and 30%. For the 2PP thermal correction model, the ratio k_s/k is the most dominant parameter of influence, with 88% to 97% of sensitivity. For the HAX thermal correction model, the S_{corr} parameter has the biggest influence for all metamodel, with an index between 46% and 61%. According to the classification made by [21], a parameter with a Sobol index above 80% is considered as "very important", while it is 'irrelevant" under 30%. Therefore, for the 2PP thermal correction model, the ratio k_s/k is a very important parameter in the sensitivity of the model.

7.5. Bayesian inversion calibration

The metamodels built serve as a foundation for the Bayesian inversion module of UQLab. The target of the calibrations is to retrieve the features of the experimental results by estimating the best roughness parameters. The calibrations carried out are listed in Tab. 5. Each calibration is performed once for the 2PP thermal correction and once for the HAX thermal correction.

Table 5. Calibrations carried out

Calibration	Metamodel used	Target of the calibration
#1	M_1	Obtain the same starting h_c value (255.1 W/m²K)
#2	M_2	Mean relative error with the experiment equal to zero

The target values (3rd column of Tab. 5) are inputted into the Bayesian module and the computation is carried out on the corresponding metamodel for each thermal correction. The calibrated roughness parameters obtained by taking the mean values given by the Bayesian solver are listed in Tab. 6. The mean values of the posterior distribution produce better results all along the channel compared to the maximum a posteriori (MAP) values. The MAP values give interesting local predictions but fails on the entire domain, as illustrated later in this section. The mean values represents a compromise to obtain satisfactory results on average on the channel's floor.

Table 6. Calibrated roughness parameters

Calibration	Calibrated parameters and MCMC sampler used*	
	HAX	2PP
#1	*k =2.1 mm* k_s = 4.6 mm S_{corr} = 1.3 MH	*k =2.2 mm* k_s = 6.4 mm AIES
#2	*k = 1.8 mm* k_s = 5.0 mm S_{corr} = 1.3 AIES	*k = 1.6 mm* k_s = 4.2 mm AIES

**AIES: Affine invariant ensemble algorithm;*
MH: Metropolis-Hastings algorithm.

The values in Tab. 6 are different from the ones tested in the baseline simulations, what explains the poor agreement with the literature prior to the calibration. These calibrated roughness parameters are inputted into the CFD solver and the simulation is run to verify the new heat transfer obtained after calibration. Fig. 6 shows the heat transfer after calibration for the 2PP thermal correction model, and Fig. 7 for the HAX thermal correction model.

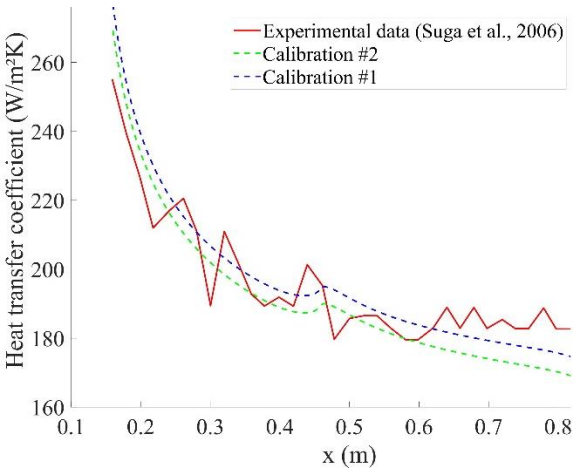

Figure 6. Heat transfer coefficient after calibration (2PP)

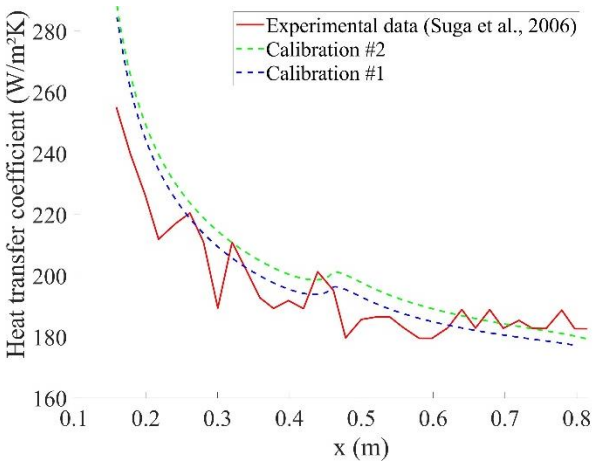

Figure 7. Heat transfer coefficient after calibration (HAX)

Fig. 6 shows that the calibrated results have a better agreement with the experimental results compared to the baseline simulation of Fig. 2. The calibration #1 for the 2PP thermal correction allows obtaining an average relative error with the experimental data of 4.7%. The calibration #2 presents similar errors with the experimental data with 4.8% of relative mean error. Globally, both calibrations for the 2PP thermal correction model are successful, showing less than 5% of error on average compared to the experimental results.

Fig. 7 shows that the calibrations for the HAX thermal correction don't give heat transfers as close to the experiments as the 2PP gave. Nevertheless, the calibration #1 for HAX presents a relative error of 7.1% with the experimental data, which is acceptable. On the other hand, the calibration #2 gives a relative error of 6.1%. Tab. 7 summarizes the relative errors obtained for each calibration. In Tab. 7, the relative errors are computed as the average for the entire rough zone among all the grid points.

Table 7. Errors with experimental data after calibration

Calibration	Average relative errors	
	HAX	2PP
#1	7.1%	4.7%
#2	6.1%	4.8%

Despite these good average results, the initial starting value of h_c for the calibration #1 is about 10% higher than the experimental one, despite being the target of the calibration. This discrepancy for the starting h_c is due to the choice of the mean value of the posterior distribution instead of the MAP for the calibrated roughness parameters. The results obtained with the calibration #1 using the MAP values are displayed on Fig. 8. For the HAX thermal correction, the MAP parameters for calibration #1 are k = 1.7 mm, k_s = 1.7 mm and S_{corr} = 1.3.

For the 2PP thermal correction, these MAP parameters are k = 3.8 mm and k_s = 4.56 mm.

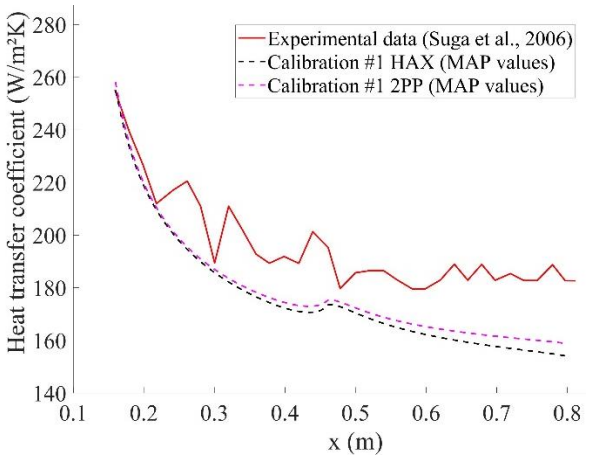

Figure 8. Calibration #1 using MAP values

Fig. 8 shows that the MAP values of the roughness parameters computed by the Bayesian solver allow recovering the correct initial value of h_c once used in the CFD solver. Nevertheless, these simulations exhibit local relative errors at the end of the channel reaching 18% for the HAX thermal correction and 16% for the 2PP correction. This shows that having the correct initial value of h_c does not guarantee a good fit all along the domain. Additionally, the experimental results uncertainty is not taken into account. The fluctuations observed on the experimental curve (in Fig. 8 for instance) indicate an uncertainty of about 6% to 10% on the experimental values. This means that the initial target value ranges roughly between 235 W/m²K and 275 W/m²K. Strictly calibrating on the plotted initial value (255.1 W/m²K) is then too restrictive and assumes there is no uncertainty on the experimental data. Thus, taking the mean values of the posterior distribution (Tab. 6) instead of the MAP is a better compromise, smoothing out the experimental errors, to obtain acceptable results in the entire domain.
Globally, the calibration procedure highlighted its suitability for the present study by allowing improving the agreement between the numerical results and the experimental data.

8. CONCLUSION

The objective of establishing a methodology to perform a calibration of roughness parameters aiming at approaching experimental heat transfers was reached. Furthermore, this methodology was applied to a curved channel test case to illustrate its capacity. Starting with an unknown experimental roughness pattern, the procedure allowed recovering roughness parameters giving less than 7.1% of discrepancies with the experimental heat transfer for the HAX thermal correction model, and less than 5% for the 2PP thermal correction model. This goal was achieved by combining the polynomial chaos expansion metamodeling with a Bayesian inversion. In the meantime, the sensitivity analysis using the Sobol sensitivity indexes highlighted that for this test case, the relation between the roughness height and the equivalent roughness plays a bigger role than the roughness height alone. Globally, the data-driven approach showed its suitability in CFD applications. In the case of unknown roughness patterns, it allows to finely select the numerical parameters to input in a CFD simulation to retrieve the experimental data. The next steps are the fine-tuning of the Bayesian approach, especially for the HAX thermal correction model, and the testing of other methodologies such as the calibration using a genetic algorithm.

9. ACKNOWLEDGEMENTS

The authors want to thank the TOMATO Association (Aéroclub de France), Paris, France, the Office of the Dean of Studies, ÉTS, Montréal, Canada, and SubstanceETS, Montréal, Canada. CFD computations were made on the supercomputer Cedar from Simon Fraser University, managed by Calcul Québec and Compute Canada.

10. REFERENCES

1. Aupoix, B. and Spalart, P.R., Extensions of the Spalart–Allmaras turbulence model to account for wall roughness. *International Journal of Heat and Fluid Flow* **2003**, *24*, No. 4, 2003, p. 454-462. doi: https://doi.org/10.1016/S0142-727X(03)00043-2.

2. Suga, K., Craft, T.J., and Iacovides, H., An analytical wall-function for turbulent flows and heat transfer over rough walls. *International Journal of Heat and Fluid Flow* **2006**, *27*, No. 5, 2006, p. 852-866. doi: https://doi.org/10.1016/j.ijheatfluidflow.2006.03.011.

3. Aupoix, B., Improved heat transfer predictions on rough surfaces. *International Journal of Heat and Fluid Flow* **2015**, *56*, No. 1, 2015, p. 160-171. doi: https://doi.org/10.1016/j.ijheatfluidflow.2015.07.007.

4. Morency, F. and Beaugendre, H., Comparison of turbulent Prandtl number correction models for

the Stanton evaluation over rough surfaces. *International Journal of Computational Fluid Dynamics* **2020**, No. 2020, p. 1-21. doi: 10.1080/10618562.2020.1753712.

5. Ignatowicz, K., Morency, F., and Beaugendre, H., Sensitivity Study of Ice Accretion Simulation to Roughness Thermal Correction Model. *Aerospace* **2021**, *8*, No. 3, 2021, p. 84. https://www.mdpi.com/2226-4310/8/3/84.

6. R. Dirling, J., *A method for computing roughwall heat transfer rates on reentry nosetips*, in *8th Thermophysics Conference*. 1973. doi: 10.2514/6.1973-763.

7. Shin, J., Characteristics of surface roughness associated with leading-edge ice accretion. *Journal of Aircraft* **1996**, *33*, No. 2, 1996, p. 316-321. doi: 10.2514/3.46940.

8. Da Ronch, A., Panzeri, M., Drofelnik, J., and D'ippolito, R., Sensitivity and calibration of turbulence model in the presence of epistemic uncertainties. *CEAS Aeronautical Journal* **2020**, *11*, No. 1, 2020, p. 33-47. doi: 10.1007/s13272-019-00389-y.

9. Marelli, S. and Sudret, B., UQLab user manual -- Polynomial chaos expansions. Chair of Risk, Safety and Uncertainty Quantification, ETH Zurich, Switzerland 2019.

10. Tabatabaei, N., Raisee, M., and Cervantes, M.J., Uncertainty Quantification of Aerodynamic Icing Losses in Wind Turbine With Polynomial Chaos Expansion. *Journal of Energy Resources Technology* **2019**, *141*, No. 5, 2019. doi: 10.1115/1.4042732.

11. P.-R. Wagner, J.N., S. Marelli, B. Sudret, UQLab user manual – Bayesian inference for model calibration and inverse problems. Chair of Risk, Safety and Uncertainty Quantification, ETH Zurich, Switzerland Zurich, Switzerland, 2021.

12. Guillas, S., Glover, N., and Malki-Epshtein, L., Bayesian calibration of the constants of the – turbulence model for a CFD model of street canyon flow. *Computer Methods in Applied Mechanics and Engineering* **2014**, *279*, No. 2014. doi: 10.1016/j.cma.2014.06.008.

13. Economon, T.D., Palacios, F., Copeland, S.R., Lukaczyk, T.W., and Alonso, J.J., SU2: An Open-Source Suite for Multiphysics Simulation and Design. *AIAA Journal* **2015**, *54*, No. 3, 2015, p. 828-846. doi: 10.2514/1.J053813.

14. Dukhan, N., Masiulaniec, K.C., Witt, K.J.D., and Fossen, G.J.V., Experimental Heat Transfer Coefficients from Ice-Roughened Surfaces for Aircraft Deicing Design. *Journal of Aircraft* **1999**, *36*, No. 6, 1999, p. 948-956. doi: 10.2514/2.2556.

15. Fortin, G., Equivalent Sand Grain Roughness Correlation for Aircraft Ice Shape Predictions. SAE International, 2019. doi: https://doi.org/10.4271/2019-01-1978.

16. Stein, M., Large sample properties of simulations using latin hypercube sampling. *Technometrics* **1987**, *29*, No. 2, 1987, p. 143-151. doi: 10.2307/1269769.

17. Schaefer, J.A., Cary, A.W., Mani, M., and Spalart, P.R., *Uncertainty Quantification and Sensitivity Analysis of SA Turbulence Model Coefficients in Two and Three Dimensions*, in *55th AIAA Aerospace Sciences Meeting*. 2017. doi: 10.2514/6.2017-1710.

18. Degennaro, A.M., Rowley, C.W., and Martinelli, L., Uncertainty Quantification for Airfoil Icing Using Polynomial Chaos Expansions. *Journal of Aircraft* **2015**, *52*, No. 5, 2015, p. 1404-1411. doi: 10.2514/1.c032698.

19. Saltelli, A., Ratto, M., Andres, T., Campolongo, F., Cariboni, J., Gatelli, D., Saisana, M., and Tarantola, S., *Global Sensitivity Analysis. The Primer*. Vol. 304. 2008. doi: 10.1002/9780470725184.ch6.

20. Prince Raj, L., Yee, K., and Myong, R.S., Sensitivity of ice accretion and aerodynamic performance degradation to critical physical and modeling parameters affecting airfoil icing. *Aerospace Science and Technology* **2020**, *98*, No. 2020, p. 105659. doi: https://doi.org/10.1016/j.ast.2019.105659.

21. Chan, K., Saltelli, A., and Tarantola, S., *Sensitivity Analysis of Model Output: Variance-based Methods Make the Difference*. 1997, 261-268. doi: 10.1109/WSC.1997.640407.